

Primary analysis of oceanic mesoscale eddies observation abilities by Sentinel-3A SRAL

YANG Jungang, ZHANG Jie, CUI Wei

First Institute of Oceanography, Ministry of Natural Resources, Qingdao 266061, China

Abstract: In this study, the north-western Pacific Ocean of Kuroshio region is selected as the experimental area to analyze the mesoscale eddies observation abilities of Sentinel-3A SRAL, including the independent detection abilities of Sentinel-3A SRAL and the improvement of mesoscale eddies detection abilities by data fusion with other satellite altimetry data. The Sentinel-3A SRAL data are mapped by the spatial-temporal objective analysis method to the sea level anomaly grid data. The mapping errors are analyzed by the comparisons between the grid data of different combinations and along the ground track of Jason-2/3. The independent detection abilities of Sentinel-3A SRAL are analyzed by the comparison between the grid data and the AVISO MSLA data. On the other hand, through the multi-satellite data fusion of different combinations of Sentinel-3A altimeter and other satellite altimeters such as Jason-2/3, the mesoscale eddies detection was performed based on the merged sea level anomaly data and the addition of Sentinel-3A SRAL data for the improvements of mesoscale eddies detection abilities by multi-satellite altimeters are concluded. It is concluded that Sentinel-3A SRAL has good abilities of mesoscale eddies detection as the combination of Jason-2 and Jason-3, and it is better than that of single altimeter of Jason-2 or Jason-3.

Key words: Sentinel-3, Altimeter, mesoscale eddy

Citation format: Yang J G,Zhang J and Cui W. 2020. Primary analysis of oceanic mesoscale eddies observation abilities by Sentinel-3A SRAL. *Journal of Remote Sensing(Chinese)*. 24(S1): 126-131

1 INTRODUCTION

Sentinel-3 is a European Earth Observation satellite mission developed to support GMES ocean, land, atmosphere, emergency, security and cryosphere applications. One of the main objectives of the Sentinel-3 mission is to measure sea surface topography with high accuracy and reliability to support ocean forecasting systems, environmental monitoring and climate monitoring. A dual-frequency (Ku and C-band) advanced Synthetic Aperture Radar Altimeter (SRAL) derived from ENVISAT RA-2, Cryosat-2 SIRAL and Jason-2/Poseidon-3, provides measurements at a resolution of approximately 300 m in SAR mode along track. Sentinel-3 uses a high inclination orbit (98.65°) for optimal coverage of ice and snow parameters in high latitudes. Sentinel-3's orbit is a near-polar, sun-synchronous orbit with a descending node equatorial crossing at 10:00 AM Mean Local Solar time. The orbital cycle is 27 days (14+7/27 orbits per day, 385 orbits per cycle). Sentinel-3A was launched on 16th February 2016 and Sentinel-3B was launched on 25th April 2018. The two in-orbit Sentinel-3 satellites enable a short revisit time (Sentinel-3 team, 2017).

Oceanic mesoscale eddy is one of important mesoscale dynamic processes in the global ocean, and it is one of the research hot-spots in physical oceanography. Mesoscale eddies play an important role in ocean circulation, material and energy transport and other marine dynamics and marine biochemical processes in the global ocean (Stammer, 1998; Chaigneau et al., 2011; Chelton et al., 2011). Mesoscale eddies usually have a spatial scale of tens to

hundreds of kilometers and a time scale of more than ten days to several months. Conventional in situ observations make it difficult to achieve complete observations of mesoscale eddies. Satellite altimetry is an important means of mesoscale eddies detection. Multi-source satellite altimetry data fusion provides abundant data for the global mesoscale eddies detection. European Space Agency (ESA) launched sentinel-3A/B satellites equipped with Synthetic Aperture Radar Altimeters (SRAL) on February 16, 2016 and April 25, 2018, which provides new data sources for the mesoscale eddies detection in global ocean. In this study, the observation abilities of mesoscale eddies by Sentinel-3A SRAL are analyzed by the comparisons between satellite altimeter data fusion of Sentinel-3A SRAL and Jason-2/3 along track data and AVISO MSLA data. In addition, the mesoscale eddies detection results by different data fusion results are also compared.

2 DATA AND METHOD

2.1 Altimeter data

Sentinel-3A SRAL data between 15 Jan. 2017 and 14 Feb. 2017 are involved in this study, and all available data of Jason-2 and Jason-3 in the same period are also used in this study. The main information of these data is shown in table 1.

The SSH data of these altimeters are used to obtain Sea Level Anomaly (SLA) which are used in the mesoscale eddies detection.

Received: 2019-10-21; **Accepted:** 2020-04-16

Foundation: Dragon 4 Project (No. 32292); Chinese National Natural Science Foundation (No.41576176).

First author biography: Yang Jungang (1980—), male, associate research fellow, His research interests are satellite altimetry data processing and their application. E-mail: yangjg@fio.org.cn.

The mean sea surface model named MSS_CNES_CLS-2011 is used in the calculation of SLA.

Table 1 The information of the used altimeter data in this study

Sensor/Satellite	Period
Sentinel-3A SRAL	Cycle013—014(2017-01-03—2017-02-26)
Jason-2	Cycle313—318(2016-12-25—2017-02-23)
Jason-3	Cycle033—037(2016-12-30—2017-02-18)

2.2 AVISO MSLA data

AVISO (Archiving, Validation and Interpretation of Satellite Oceanographic data) distributes satellite altimetry data which include AVISO global sea surface height products such as gridded sea level anomalies. The Copernicus Marine and Environment Monitoring Service (CMEMS) has taken over the whole processing and distribution of those products (formerly distributed by Aviso+ with no changes in the scientific content). The AVISO MSLA data on 30th January 2017 is used in this study. This AVISO product merged the data of Altika Drifting Phase, Cryosat-2, HY-2A Geodetic Phase, Jason-3, OSTM/Jason-2 Interleaved and Sentinel-3.

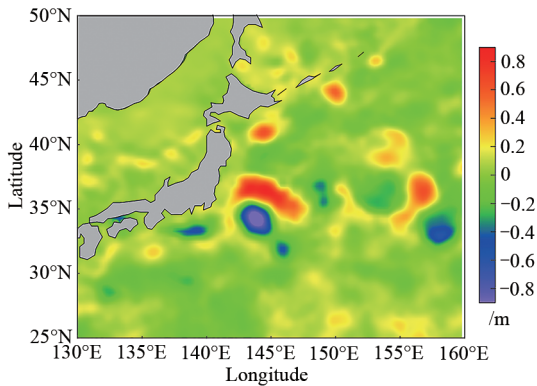


Fig.1 The AVISO MSLA distribution in the study area

2.3 Spatial-temporal objective analysis method

Spatial-temporal Objective Analysis is one method to map the irregular measurement data. Mapping of SLA with the objective analysis method is to determine the value of the SLA field at each grid point in time and space according to the given various measurements of the field unevenly spread over time and space (Tran & Dibarbouré, 1999). Set $h(\vec{x})$ is the SLA at the grid point \vec{x} which is expected to be obtained. $H_{obs}^i(\vec{x}_i)$ ($i = 1, 2, \dots, N$) are SLAs at the point \vec{x}_i along the ground track of altimeters. Based on N observed SLAs, the SLA grid data are calculated by the following expression.

$$h(\vec{x}) = \sum_{j=1}^N C_{sj} \left(\sum_{i=1}^N A_{ij}^{-1} H_{obs}^i \right) \quad (1)$$

Where, A is the covariance matrix for the observations themselves. C is the covariance vector for the observations and the field to be estimated. H_{obs}^i is regarded as the sum of real SLA value H^i and observed error ε_i .

$$H_{obs}^i = H^i + \varepsilon_i \quad (2)$$

The covariance matrices A and C are

$$A_{ij} = \langle H_{obs}^i H_{obs}^j \rangle = F(\vec{x}_i - \vec{x}_j) + \langle \varepsilon_i \varepsilon_j \rangle \quad (3)$$

$$C_{sj} = \langle h(\vec{x}) H_{obs}^j \rangle = \langle h(\vec{x}) H^j \rangle = F(\vec{x} - \vec{x}_j) \quad (4)$$

The associated error variance e^2 is given by

$$e^2 = C_{xx} - \sum_{i=1}^n \sum_{j=1}^n C_{xi} C_{xj} A_{ij}^{-1} \quad (5)$$

The error covariance $\langle \varepsilon_i \varepsilon_j \rangle = \delta_{ij} b^2$ for points (i, j) not on the same track or in the same cycle, and $\langle \varepsilon_i \varepsilon_j \rangle = \delta_{ij} b^2 + E_{LW}$ for points (i, j) on the same track or in the same cycle. Where, b^2 is the variance of the white measurement noise and E_{LW} is the variance of the long-wavelength error.

The spatial - temporal correlation function $F(r, t)$ of the sea level anomaly field is given by

$$F(r, t) = \left(1 + ar + \frac{(ar)^2}{6} - \frac{(ar)^3}{6} \right) \exp(-ar) \exp(-t^2/T^2) \quad (6)$$

Where r is distance, T is time, L is the spatial correlation scale, and T is the temporal correlation scale. In this study, L and T are set at 150 km and 15 days, respectively, which are typical scales of the mesoscale eddy in the study area.

2.4 Mesoscale eddies detection method

a winding-angle method (Sadarjoen & Post, 2000) is used in the mesoscale eddy detection in this study. First of all, a cyclonic/anticyclonic possible center of mesoscale eddies is determined through searching the local SLA minimum or maximum in a moving window of $1^\circ \times 1^\circ$. Then for each local SLA minimum or maximum, the closed SLA contour is increased/decreased with an amplitude of 1 cm in the process until the closed contour is maximum/minimum. The outermost closed contour encircling only one cyclonic/anticyclonic center is taken into account as the eddy edge. an eddy is defined as a simply connected set of pixel grids that satisfying the following criteria (Cui, et al, 2016): (1) The SLA values of all pixels are below/above the SLA edge threshold for the cyclonic/anticyclonic eddies; (2) There are at least eight pixels and fewer than 1000 pixels comprising the connected region; (3) There is one local minimum/maximum of SLA for the cyclonic/anticyclonic eddies; (4) The amplitude of the eddy is at least 3 cm; (5) The distance between any pair of pixels within the eddy must be less than 600 km.

3 ANALYSIS OF MESOSCALE EDDIES OBSERVATION ABILITIES

The along-track Sea Level Anomaly (SLA) data of Jason-2/3 and Sentinel-3A SRAL are calculated according to their GDR data, and the mean sea surface model named MSS_CNES_CLS-2011 is used in this calculation. The along-track SLA data of Sentinel-3A SRAL are mapped to gridded SLA data alone and by the different combinations of different altimeters using the spatial-temporal objective analysis method introduced in section 2. Then the SLA grid data are used to analyze mesoscale eddies observation abilities. The SLA grid data on 30 January 2017 is calculated and used to analyze the mesoscale eddies observation abilities by Sentinel-3A SRAL. The analysis of mesoscale eddy observation abilities of Sentinel-3A SRAL includes three parts: the comparisons of differences between grid SLA data of different altimeters' combinations and AVISO MSLA data; the comparisons of grid SLA data with along the track of Jason-2/3 data which are taken as the 'truth'; the comparisons of mesoscale eddies detection results of different grid SLA data. Fig.2 is the sketch map of the along-track SLA distribution of Jason-2/3, Sentinel-3A SRAL.

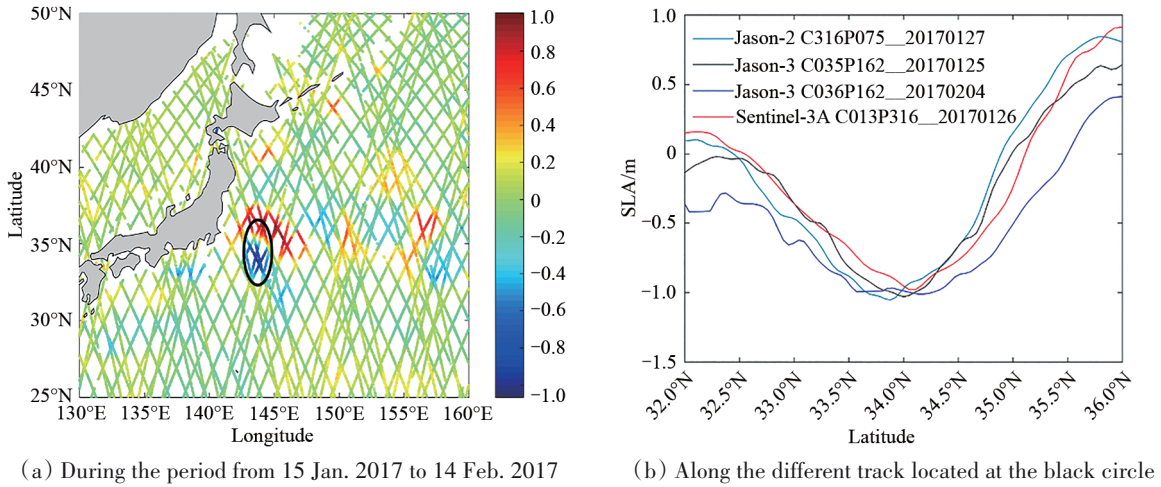


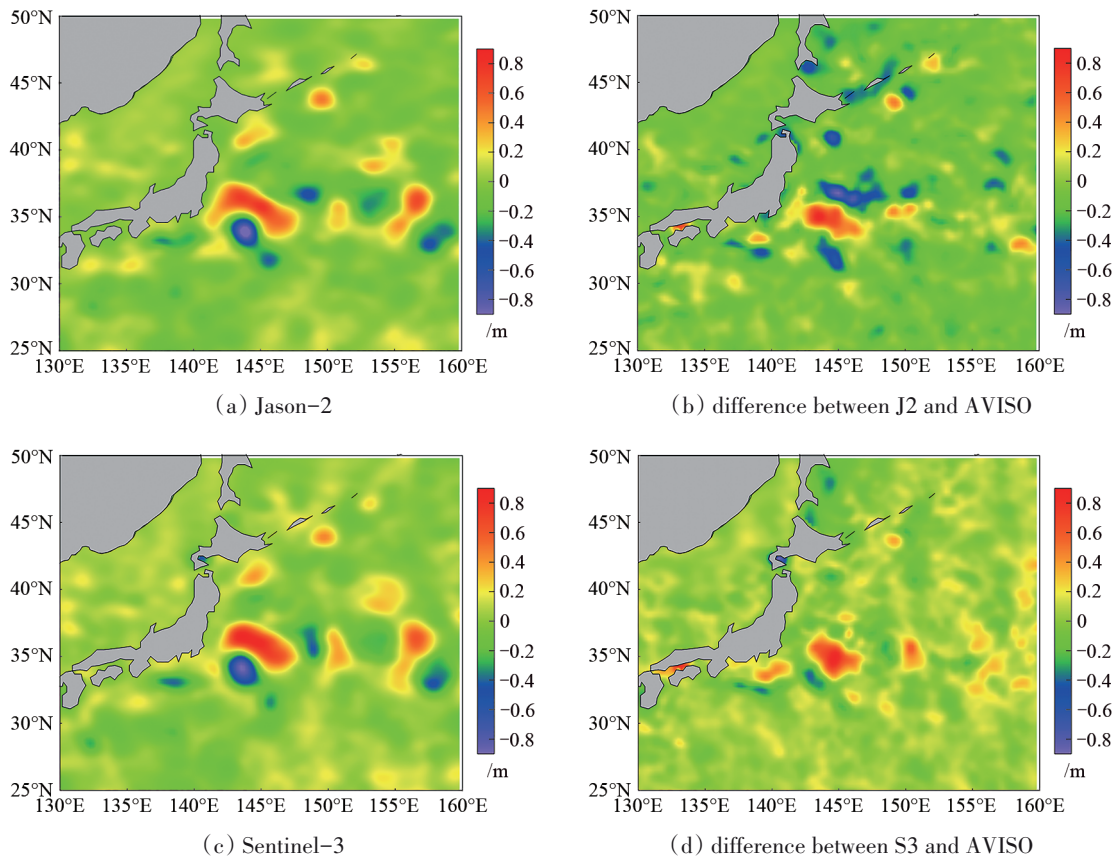
Fig. 2 SLA distribution of Jason-2/3, Sentinel-3A SRAL

3.1 Comparisons of grid SLA data of different combinations and AVISO MSLA data

In order to analyze the mesoscale eddies observation abilities of Sentinel-3A SRAL, the grid SLA data of different altimeter combinations which include that of Sentinel-3A SRAL (S3), Jason-2 (J2), Jason-2 & Jason-3 (J2+J3), Jason-2 & Sentinel-3A SRAL (J2+S3) are compared to the AVISO MSLA data on 30 January 2017. The distribution of grid SLAs of different altimeter combinations

and their differences between grid SLA data and AVISO MSLA are shown in Fig. 3. It is shown that grid SLA data of S3 and J2+S3 is better than that of J2 and J2+J3. This means Sentinel-3A SRAL has good observation ability of SLA.

In order to analyze the mesoscale eddies detection ability of Sentinel-3A SRAL quantitatively, the RMS of the differences between grid SLA data of the different altimeter combinations and AVISO MSLA data is calculated and given in Fig. 4.



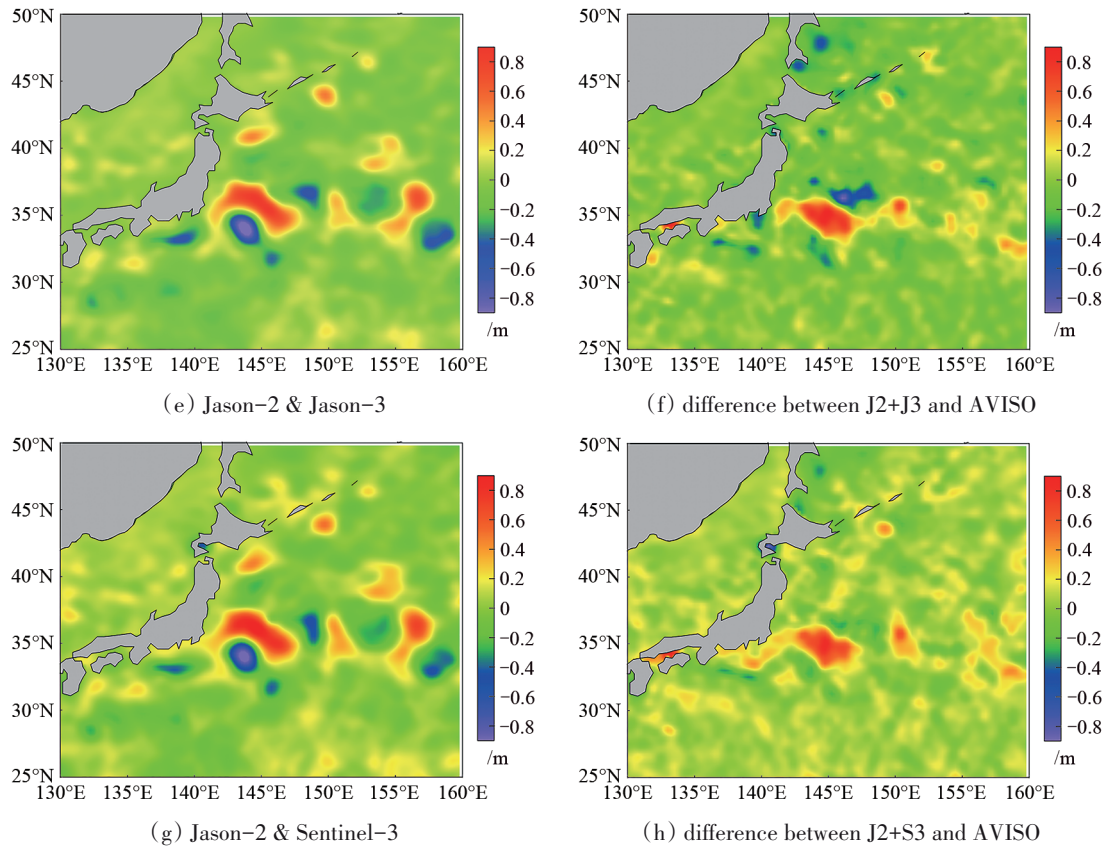


Fig. 3 Grid SLA distribution of different altimeter combinations and their differences with AVISO MSLA

It is shown in Fig. 4 that the grid SLA data of J2+S3 has the least RMS and the RMS is $J2+S3 < S3 < J2+J3 < J2$. The combination of Jason-2 and Jason-3 improve the mesoscale eddies observation ability of Jason-2. Sentinel-3A SRAL has the better mesoscale eddies observation ability than that of Jason-2 and the combination of Jason-2 and Jason-3. The combination of Sentinel-3A SRAL and Jason-2 has the best mesoscale eddies observation ability between these cases. This means that the Sentinel-3A SRAL has good mesoscale eddies observation ability.

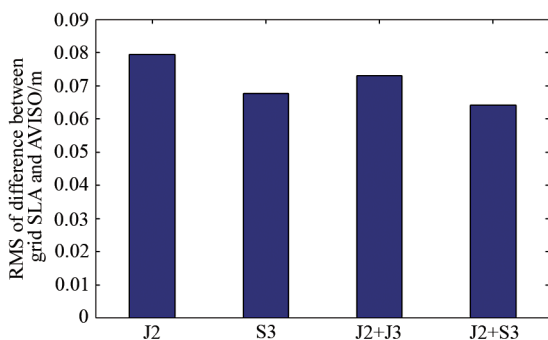


Fig. 4 RMS of the difference between grid SLA data and AVISO MSLA data

3.2 Comparisons to independent data

In the above analysis, AVISO MSLA data are taken as the 'truth' SLA data and used to analyze the mesoscale eddies observation ability of different altimeter combination. In this section, the along

track data of Jason-2/3 are taken as the 'truth' of ocean (Dibarbour et al., 2012). The mesoscale eddies observation of Sentinel-3A SRAL is analyzed by the comparisons between the grid SLA data of S3 and J2+S3 along Jason-3 track and the comparisons between the grid SLA data of S3 and J2+S3 along Jason-2 track. The difference between grid SLA data of S3 and J2+S3 along Jason-3 track and the RMS of improvement are given in table 2.

It can be seen in table. 2 that the addition of Sentinel-3A SRAL data improves the SLA observation ability of Jason-2 grid SLA data. The average RMS of improvement is 0.96 cm. the comparisons between grid SLA data of J3 and J3+S3 along ground track of Jason-2 show the average RMS of improvement is 0.99 cm. It means the addition of Sentinel-3A SRAL data to Jason-2 or Jason-3 can improve the precision of grid SLA data and the mesoscale eddies observation ability.

3.3 Comparisons of mesoscale eddies detection results by different grid SLA data

In order to analyze the mesoscale eddies detection ability of Sentinel-3A SRAL, the grid SLA data of different altimeter combinations on 30 January 2017 are used to mesoscale eddies detection by the method introduced in section 4.2. the mesoscale eddies detection results are shown in Fig. 5.

Fig.5 (a), (b) and (c) are the detection results of mesoscale eddies by the combination of Jason-2 and Jason-3, Sentinel-3A, and the combination of Jason-2 and Sentinel-3A. The mesoscale eddies detection abilities of these three cases are analyzed by comparing to the mesoscale eddies detection results of AVISO MSLA data and artificial cognition of mesoscale eddies. Three representative regions of the study area are analyzed to compare the mesoscale ed-

dies detection ability. In rectangular region, there are many little eddies in Fig. 5(a) which is more than that of Fig. 5(b) and (c). This is due to the existence of some false information of eddies in Fig. 5(a). The mesoscale eddies detection results of Sentinel-3A and the combination of Jason-3 and Sentinel-3A are better than those of the combination of Jason-2 and Jason-3. In circular region, an anticyclonic eddy is identified by Sentinel-3A and the combination of Jason-3 and Sentinel-3A, but it isn't identified by the combination of Jason-2 and Jason-3. It implies that the addition of Sentinel-3 increases the mesoscale eddy observation ability. In elliptical region,

the detection results of Sentinel-3A and the combination of Jason-2 and Sentinel-3A have fewer little eddies than those of the combination of Jason-2 and Jason-3, and this is close to the results of AVISO MSLA and artificial cognition of eddies. In general, it can be seen that the mesoscale eddies detection results of S3 and J2+S3 have larger eddies which are closer to the real ocean than that of J2. It means that the Sentinel-3A SRAL has better mesoscale eddies observation ability than Jason-2, and the combination of Jason-2 and Sentinel-3A SRAL improves their mesoscale eddies observation ability.

Table 2 Differences between grid SLA data of S3 and J2+S3 and the RMS of improvement

Cycle	Pass	Age	Difference between grid data and actual measurements /m		RMS of improvement /m
			S3	J2+S3	
35	151	5	0.107	0.098	0.006
35	160	5	0.078	0.077	0.006
35	162	5	0.071	0.063	0.012
35	177	4	0.088	0.077	0.011
35	186	4	0.080	0.062	0.014
35	201	3	0.059	0.049	0.011
35	203	3	0.077	0.062	0.013
35	212	3	0.075	0.064	0.01
35	227	2	0.065	0.058	0.006
35	238	2	0.076	0.059	0.016
35	253	1	0.072	0.065	0.006
36	8	1	0.078	0.062	0.009
36	10	1	0.065	0.057	0.007
36	23	0	0.074	0.07	0.007
36	25	0	0.059	0.058	0.005
36	34	0	0.073	0.064	0.007
36	49	1	0.113	0.1	0.014
36	51	1	0.055	0.053	0.015
36	60	1	0.108	0.096	0.008

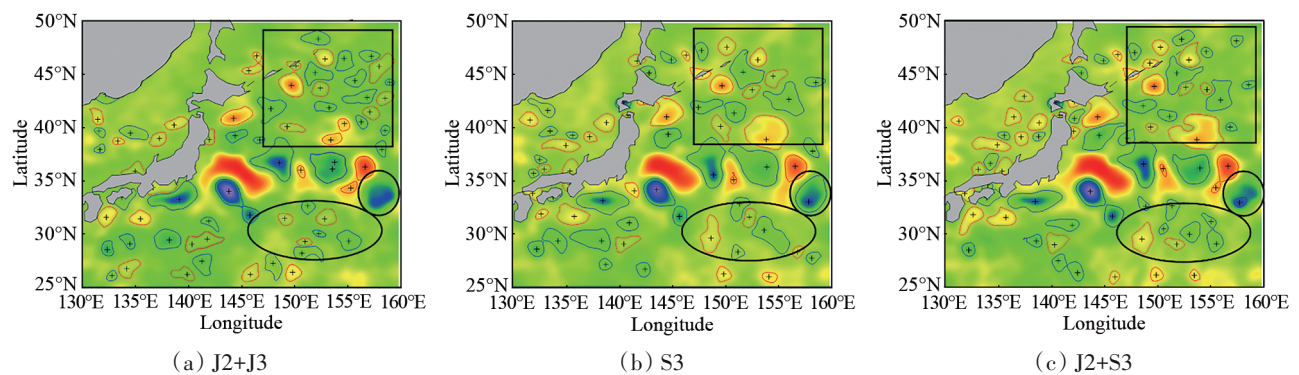


Fig. 5 Mesoscale eddies detection results of different grid SLA data

4 CONCLUSIONS

Sentinel-3A SRAL is the new generation satellite altimeter of European Space Agency, and it supplies one new kind of altimetry

data with smaller track spacing and larger spatial coverage for the global ocean monitoring. In this study, the north-western Pacific Ocean of Kuroshio region is selected as the experimental area and the mesoscale eddies observation abilities of Sentinel-3A SRAL

are analyzed. Firstly, Sentinel-3A SRAL data are used in the mapping of SLA data with different altimeters combination to analyze the mesoscale eddies observation ability of Sentinel-3A SRAL by the comparison between the grid SLA data and the AVISO MSLA data, which includes the independent detection abilities of Sentinel-3 SRAL and the improvement of mesoscale eddies detection abilities by data fusion with other satellite altimetry data. Furthermore, the mapping errors are analyzed by the comparisons to the Jason-2/3 track data which are taken as the 'truth' ocean. Lastly, the mesoscale eddies detection results of different grid SLA data of the different altimeters combination are compared to analyze the mesoscale eddies observation ability of Sentinel-3A SRAL. Finally, it is concluded that Sentinel-3A SRAL has good abilities of mesoscale eddies detection as the combination of Jason-2 and Jason-3, and it is better than that of single altimeter of Jason-2 or Jason-3. The addition of Sentinel-3A SRAL to Jason-2 or Jason-3 improves the mesoscale eddies observation ability effectively. It is believed that the combination of Jason-2/3 and Sentinel-3A SRAL will obtain the best mesoscale eddies detection results.

Sentinel-3 Team. Sentinel-3 User Handbook. GMES-S3OP-EOPG-TN-13-000. 13th January 2017, <https://sentinel.esa.int/> [2019-10-21].

REFERENCES

- Stammer D. 1998. On eddy characteristics, eddy transports, and mean flow properties. *Journal of Physical Oceanography*, 28: 727-729.
- Chaigneau A, Le Texier M, Eldin G, Grados C and Pizarro O. 2011. Vertical structure of mesoscale eddies in the eastern south Pacific Ocean: a composite analysis from altimetry and Argo profiling floats. *Journal of Geophysical Research*, 116, C11025, doi: 10.1029/2011JC007134.
- Chelton D B, Schlax M G and Samelson R M. 2011. Global observations of nonlinear mesoscale eddies on near-surface oceanic chlorophyll. *Science*, 334: 328-332.
- Traouk P Y L and Dibarboure G. 1999. Mesoscale Mapping Capabilities of Multiple-Satellite Altimeter Missions. *Journal of Atmospheric & Oceanic Technology*, 16 (9): 1208-1223.
- Sadarjoei I A and Post F H. 2000. Detection, quantification and tracking of vortices using streamline geometry. *Computers & Graphics*, 24: 333-341. DOI: 10.1016/S0097-8493(00)00029-7.
- Cui W, Yang J G and Ma Y. 2016. A statistical analysis of mesoscale eddies in the Bay of Bengal from 22-year altimetry data. *Acta Oceanol. Sin.*, 35 (11): 16-27.
- Dibarboure G, Renaudie C, Pujol M I, et al. 2012. A demonstration of the potential of Cryosat-2 to contribute to mesoscale observation. *Advances in Space Research*, 50(8):1046-1061.